Biomaterials 33 (2012) 464–472

Contents lists available at SciVerse ScienceDirect

Biomaterials

journal homepage: www.elsevier.com/locate/biomaterials

Formation of post-confluence structure in human parotid gland acinar cells on PLGA through regulation of E-cadherin

Yen-Hui Chan[a], Tsung-Wei Huang[b,c], Ya-Shuan Chou[a], Sheng-Hao Hsu[d], Wei-Fang Su[d,e], Pei-Jen Lou[f,**], Tai-Horng Young[a,d,*]

[a] Institute of Biomedical Engineering, College of Medicine and College of Engineering, National Taiwan University, No. 1, Sec. 1 Jen-Ai Road, Taipei 100, Taiwan
[b] Department of Otolaryngology, Far Eastern Memorial Hospital, Taipei, Taiwan
[c] Department of Health Care Ministration, Oriental Institute of Technology, Taipei, Taiwan
[d] Institute of Polymer Science and Engineering, College of Engineering, National Taiwan University, Taipei, Taiwan
[e] Department of Material Science and Engineering, College of Engineering, National Taiwan University, Taipei, Taiwan
[f] Department of Otolaryngology, National Taiwan University Hospital and College of Medicine, 7, Chung-Shan South Road, Taipei, Taiwan

ARTICLE INFO

Article history:
Received 27 June 2011
Accepted 23 September 2011
Available online 10 October 2011

Keywords:
Poly (lactic-co-glycolic acid) (PLGA)
Human parotid gland acinar (PGAC) cells
Post-confluence structure (PCS)
E-cadherin

ABSTRACT

As a potential solution for patients to retrieve their lost salivary gland functions, tissue engineering of an auto-secretory device is profoundly needed. Under serum-free environment, primary human parotid gland acinar (PGAC) cells can be obtained. After reaching confluence, PGAC cells spontaneously form three-dimension (3D) cell aggregations, termed post-confluence structure (PCS), and change their behaviors. Poly (lactic-co-glycolic acid) (PLGA) has been widely used in the field of biomedical applications because of its biodegradable properties for desired functions. Nonetheless, the role of PLGA in facilitating PGAC cells to form PCS has seldom been explored to recover epithelial characteristics. In this study, PGAC cells were found to have a greater tendency to form PCS on PLGA than on tissue culture polystyrene (TCPS). By tracing cell migration paths and modulating E-cadherin activity with specific inhibitor or antibody, we demonstrated that the static force of homophilic interaction on surfaces of individual cells, but not the dynamics of cell migration, played a more important role in PCS formation. Thus, PLGA was successfully confirmed to support PGAC cells to form more PCS through the effects on enhancing E-cadherin expression, which is associated with FAK/ILK/Snail expression in PGAC cells. This result indicates that selective appropriate biomaterials may be potentially useful in generating 3D PCS on two-dimension (2D) substrate without fabricating a complex 3D scaffold.

1. Introduction

Irreversible damage of salivary glands is a common side effect caused by radiation therapy for the patients suffered from head and neck cancer, which leads to a persistent salivary hypofunction with marked reductions in salivary output [1]. At present, there is no effective therapy for this condition. Much effort has focused on implementing tissue engineering principles to develop an artificial SG device for the replacement of destroyed glands [2–12]. The most challenging part of human salivary gland tissue engineering is the paucity of cells. Therefore, some investigators established proper cell lines for such purpose [2–4]. In our laboratory, we focused on primary culture and set up a stable protocol to harvest multiple cell types from human parotid gland tissues [5]. By using the low-calcium and serum-free culture method, parotid gland acinar cells (PGAC cells) could be greatly expanded with high purity [5]. In addition, human salivary gland epithelial cells are at highly differentiated status so it is difficult to enrich the amount of primary cells and to characterize the physiological property of cultured cells. In theory, function recovery of gland type cells could be expected through the help of 3D culture methods such as fabricating of scaffolds. However, even without 3D scaffolds, it has been reported that rat salivary gland-derived cells could form cell aggregations during 2D culture and change their functions [13]. In our previous study, we also observed that human PGAC cells automatically form 3D aggregations (termed PCS, post-confluence structure) to exhibit higher expression levels and different location patterns of function-related proteins [14]. Actually, we have observed aggregative behavior of several types of cells when they were maintained on

* Corresponding author. Institute of Biomedical Engineering, College of Medicine and College of Engineering, National Taiwan University, No. 1, Sec. 1 Jen-Ai Road, Taipei 100, Taiwan. Tel.: +886 2 23123456x81455; fax: +886 2 23940049.
** Corresponding author. Tel.: +886 2 23123456x65224; fax: +886 2 23410905.
E-mail addresses: pjlou@ntu.edu.tw (P.-J. Lou), thyoung@ntu.edu.tw (T.-H. Young).

0142-9612/$ – see front matter © 2011 Elsevier Ltd. All rights reserved.
doi:10.1016/j.biomaterials.2011.09.060

certain biomaterial surfaces in specified conditions. For example, tooth germ cells spontaneously grow into floating spheroids when they are seeded on poly vinyl alcohol (PVA) [15]. Melanocytes can be cultured into adherent spheroids on chitosan [16]. Dermal papilla cells can self-assembly into many compact spheroidal microtissues on poly (ethylene-co-vinyl alcohol) (EVAL) [17].

The present study aims to disclose a simple means to generate more 3D salivary gland cultures that can help cells to retrieve their functions without fabricating complex 3D scaffolds. To this end, we cultivated PGAC cells on different biomaterials to observe different cell aggregating behaviors. These results implied the feasibility of controlling PCS formation by manipulating substrate properties of biomaterials. Since E-cadherin plays a key role in cell adhesion, this study further investigated the involvement of E-cadherin in PCS formation and tried to characterize the possible molecular regulating mechanism. To our knowledge, PGAC cells were not employed to examine how E-cadherin can be triggered by biomaterials. Our findings show poly (D,L-lactide-co-glycolide) (PLGA) is an effective substrate that promotes PCS formation and the E-cadherin-dependent pathway plays an important role in mediating function of PGAC cells.

2. Materials and methods

2.1. Cell culture and assays for PCS formation, migration, and attachment

Human parotid gland (HPG) tissues were obtained from patients during surgery. The study procedures were approved by the Institutional review Board of National Taiwan University Hospital. The specimens were kept in cold phosphate-buffered saline (PBS) and immediately transferred to laboratory. The specimens were washed with ice cold PBS containing 2% antibiotics (penicillin 200 μg/ml, streptomycin 200 μg/ml, and amphotericin B 0.5 μg/ml) to clean the surface, with all blood or other undesirable substances removed. Then all connective tissues were carefully removed from the specimens using fine forceps and scissors, leaving only the shallow-yellow acinar tissue explants. The explants were minced with fine scissors to a size of less than 0.5 mm^3, and then enzymatically treated with collagenase B (Roche Diagnostics GmbH, Mannheim, Germany), elastase (Roche Diagnostics GmbH, Mannheim, Germany), and DNase I (Roche Diagnostics GmbH, Mannheim, Germany) at 37 °C for 30 min with gently shaken by orbital shaker at the speed of 50 rpm. The digested tissue solution was filtered through 100 μm cell strainer and pooled into a 50 ml centrifuge tube, then centrifuged at 300 g for 5 min. Finally, the supernatant was discarded and the cell pellet was resuspended in keratinocyte serum free medium (K-SFM) (Invitrogen, Carlsbad, CA) containing 5 ng/ml epidermal growth factor and 50 μg/ml bovine pituitary extract (BD, U.S.A), then seeded homogenously at the density of 5×10^6 cells in 25 cm^2 culture flask. The incubator was set at 37 °C in 5% CO_2. Treated cell viability was determined via Trypan blue staining to ensure it exceeded 80%. To eliminate unknown effects, no antibiotics were added to the culture medium.

The PCSs used for series assays were using the cells of passage 1 that have been primarily cultured (defined as passage 0) in flask within 2 weeks before they reach confluence. The cells looked homotypical and did not form PCS. In the assay of evaluating PCS formation tendency, the cells were seeded at the density of 1×10^5 cells/cm^2. In Src inhibitor and anti-E-cadherin additive assays, the cells were seeded at the density of 1×10^4 cells/cm^2 to avoid instant formation of PCS causing by confluence state. The addition of anti-E-cadherin was at the concentration of 50 μg/ml.

To quantify the PCS formation, the cell images were acquired under the light microscopy Zeiss Axiovert 200 inverted microscope (Carl Zeiss, Germany). The images of PCSs were manually labeled from at least 10 views by 3 experienced people and quantified by ImageJ software. The cell migration was using the time-lapse microscopy to acquire time series cell images with 10 min interval and total 10 h duration. The cell tracks and velocity were analysis by ImageJ. The cell attachment assay was carried out by 0.25% trypsin-EDTA solution (Sigma, MO) to detach the cells from the substrate.

2.2. Preparation of the PLGA membrane

PLGA (lactide:glycolide 75:25), molecular weightt 66,000–107,000 was purchased from Sigma–Aldrich (St. Louis, MO). PLGA casting membrane was prepared as follows: PLGA was dissolved in chloroform at 1% w/w, and the polymer solution was spread on glass plate in a thickness of 500 μm and evaporated at 35 °C for 24 h. The residual solvent in the membrane was wash by series of washing steps. Before cell culture, the membrane was sterilized by 75% alcohol and washed by PBS.

2.3. Semi-quantitative reverse-transcription polymerase chain reaction (RT-PCR)

Total RNA was extracted from tissue and cultured cells using Trizol® reagent (Invitrogen, Carlsbad, CA) and reverse-transcribed with Transcriptor High Fidelity cDNA Synthesis Kit (RocheDiagnostics GmbH, Mannheim, Germany) according to the instructions of the manufacturer. The 260/280 ratios of extracted RNA were all above 1.9. PCR was carried by using SuperScript® III Reverse Transcriptase (Invitrogen, U.S.A) and the primers: E-cadherin: Forward: 5′-AAG-GTG-ACA-GAG-CCT-CTG-GAT-AGA-3′, Reverse: 5′-TCT-GAT-CGG-TTA-CCG-TGA-TCA-A-3′; α-amylase: forward: 5′-AAT-TGA-TCT-GGG-TGG-TGA-GC, reverse: 5′-CTT-ATT-TGG-CGC-CAT-CGA-TG-3′; AQP5: Forward: 5′-CAA-GGC-CGT-GTT-CGC-AGA-GTT-CT-3′, Reverse: 5′-TCT-TCC-GCT-CTT-CCC-GCT-GCT-CC-3′; ZO-1: Forward: 5′-CGG-TCC-TCT-GAG-CCT-GTA-AG-3′, Reverse: 5′-GGA-TCT-ACA-TGC-GAC-GAC-AA-3′. GAPDH: Forward: 5′-GGA-AGG-TGA-AGG-TCG-GAG-TC-3′, Reverse: 5′-CAG-TAG-AGG-CAG-GGA-TGA-TG-3′.

2.4. Western blot

Cultured cell and gland tissue lysates were obtained by using RIPA lysis buffer containing the Complete™ protease inhibitor cocktail and PhosSTOP Phosphatase Inhibitor Cocktail (RocheDiagnostics GmbH, Mannheim, Germany) to avoid the protein degradation. Following centrifugation at 15,000 g for 30 min, the supernatant was transferred into pre-cooled fresh 1.5 ml eppendorf tubes, then 3 μl of each sample solution was used for protein quantification by the Quant-iT™ Assay System (Invitrogen, Carlsbad, CA). The protein samples were denatured and separated by sodium dodecyl sulfate-polyacrylamide gel electrophoresis (SDS-PAGE) and transferred onto the Immobilon-P (Millipore) membrane by a semidry system. Following blocking in 2.5% bovine serum albumin (overnight at 4 °C), the membranes were probed with primary antibodies at room temperature for 2 h, washed and incubated in HRP-conjugated secondary antibodies and, finally, visualized by enhanced chemiluminescence (ECL) (Millipore, Billerica, MA). The antibodies used: anti-intergrin β1 (BD, U.S.A), anti-p-FAK (Millipore, U.S.A), anti-FAK (Abcam, UK), anti-ILK (Millipore, U.S.A), anti-Snail (Abcam, UK), anti-β-actin (Millipore, U.S.A), anti-p-Src (Abcam, UK), anti-Src (Abcam, UK), anti-fibronectin (Santa Cruz, U.S.A).

2.5. Immunofluorescense microscopy

Cultured cells were washed with ice cold PBS and immediately fixed with 4% PFA/PBS, permeabilized with 0.2% Triton X-100/4% PFA/PBS. Following fixation and permeabilization, samples were blocked in 1% bovine serum albumin (BSA)/PBS at 4 °C overnight, then probed with primary antibodies. The labels were visualized using Alexa Fluor-labeled secondary antibodies (Alexa Fluor 488 and Alexa Fluor 568, Invitrogen, U.S.A). Immunofluorescent images were obtained using Zeiss Axiovert 200 inverted microscope (Carl Zeiss, Germany) or Leica TCS SP5 confocal spectral microscope imaging system (Leica, Germany). The antibodies used: anti-AQP-3 (Calbiochem, Germany), anti-ZO-1 (BD, U.S.A), anti-E-cadherin (BD, U.S.A), anti-vinculin (Millipore, U.S.A), rodamine-phalloidin (Millipore, U.S.A), DAPI (Millipore, U.S.A).

The focal adhesion structures of PGAC cells on PLGA and TCPS were observed with the actin cytoskeleton/focal adhesion staining kit (Millipore, U.S.A). The actin filaments were labeled by TRITC-conjugated phalloidin, and the Vinculin molecules were labeled by anti-Vinculin antibody. The fluorescence images were scanned by the confocal microscopy.

2.6. Scanning electron microscopy

The prepared PLGA membrane and TCPS were placed in vacuum for 24 h and then sputtered with gold. Images were acquired by scanning electron microscope (Hitachi S-2400).

2.7. Protein adsorption analysis

The 10 μg/ml human fibronectin (BD, U.S.A) solution was used to perform the 5 μg/cm^2 coating of substrates. After 48 h of incubation, the residual solution was discard and the substrates were washed by PBS for three times. The 2% sodium dodecyl sulfate (SDS) solution was used to collect the adsorpted protein on the substrates and then analyzed by Western blot.

2.8. Statistics

Results were observed in three independent experiments from different subjects. Data were expressed as mean ± standard deviation (SD). Differences between groups were compared using *t*-test. A p value <0.05 indicated a significant difference.

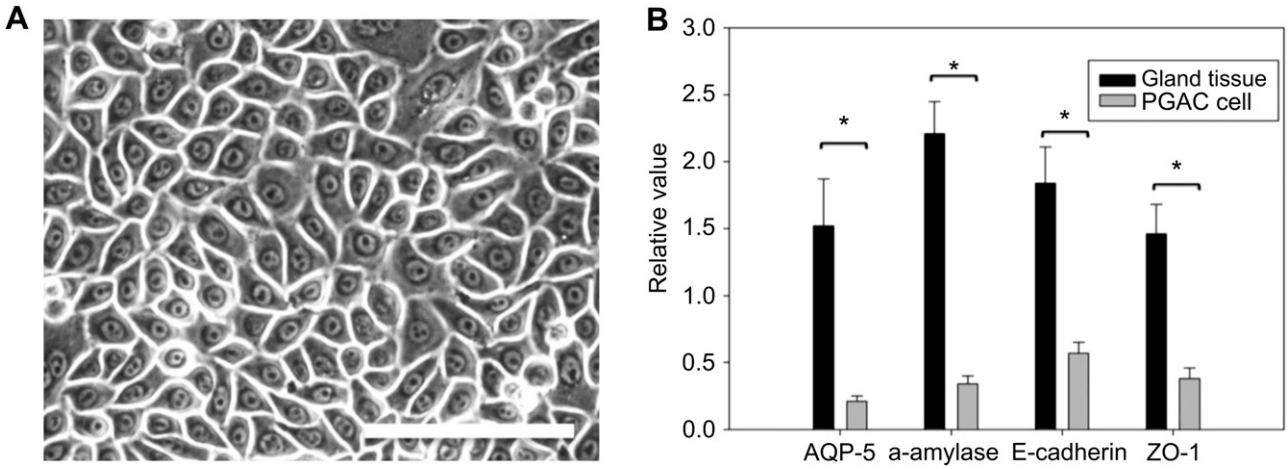

Fig. 1. Primary cultured PGAC cells and their mRNA expressions. (A) The polygonal epithelial cells expanded as a monolayer (bar: 100 μm) at day 14 of primary culture. (B) The mRNA expression comparison of function-related proteins AQP-5, α-amylase, E-cadherin, and ZO-1 between PGAC cells and gland tissue.

3. Results

3.1. PCS formation and function recovery of PGAC cells on TCPS

After isolation from gland tissue, PGAC cells on TCPS could be selectively expanded from mixed gland cells by using K-SFM-based medium [5]. Under the serum-free and low-calcium environment, PGAC cells expanded with a homogeneous morphology (Fig. 1A) but lacked cell–cell adhesion structures such as tight junction [5]. Compared to the gland tissue, the mRNA expression of functional-related proteins was greatly decreased (Fig. 1B), revealing that cultured PGAC cells with a monolayer structure are in a dedifferentiation status [14].

After reaching the confluence, PGAC cells spontaneously formed three-dimension PCSs (Fig. 2A). Cells in PCS obviously changed AQP-3 and ZO-1 expression pattern compared to cells within two-dimension monolayer structure (Fig. 2B) [14]. This phenomenon implies that cell physiology was greatly affected during the formation of PCS. In Fig. 2C, the expression of integrin β1 and E-cadherin of PGAC cells in PCS was obviously increased compared to those in two-dimension cells. The integrin β1 even showed a molecule weight shift in two-dimension cultured cells and returned to the same level of the tissue after the PCS formation, implying that the PCS was more similar to the in vivo environment.

3.2. PCS formation of PGAC cells on PLGA

After 3 days of culture, PGACs at the seeding density of 1×10^5 cells/cm^2 also could grow into compact PCSs on PGLA (Fig. 3A). Comparing the formation of PCSs on PGLA with TCPS at the same seeding density and culture time, the average size of PCSs on PLGA was about two times larger than on TCPS (Fig. 3B), and the

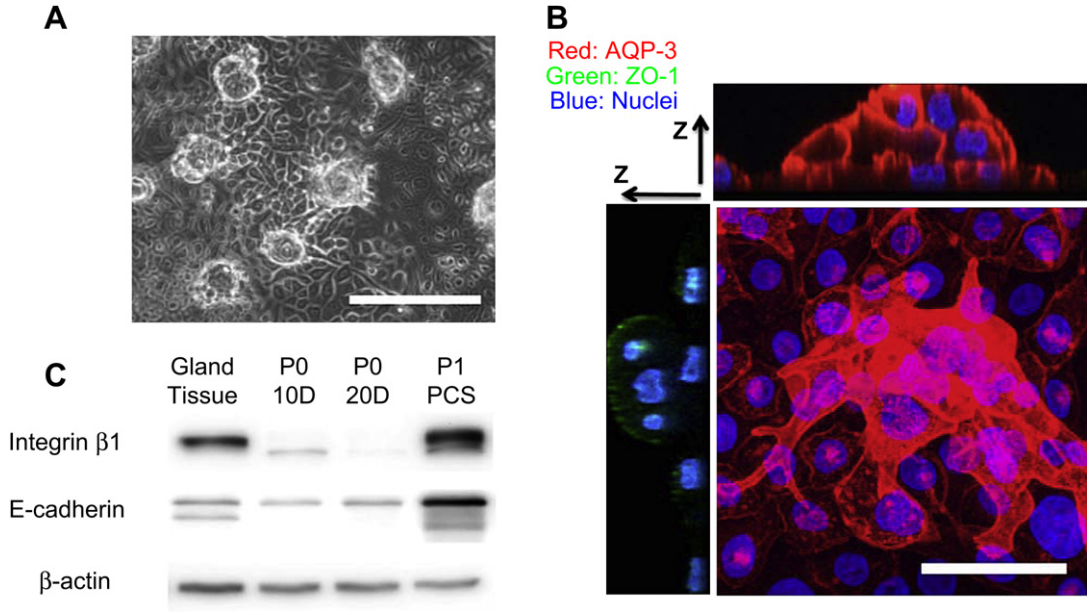

Fig. 2. The post-confluence structures (PCSs). (A) The PCSs observed in confluent region at day 21 of primary culture (bar: 100 μm). (B) Immunostaining of AQP-3 (red) and ZO-1 (green) in PCS. Both AQP-3 and ZO-1 molecules showed a different expression pattern in PCS compared to the periphery 2D cells (bar: 25 μm). (C) The Western blot analysis of protein expression change of integrin β1 and E-cadherin from gland tissue, passage 0 (P0) cells at 10 days and 20 days culture, and cells with PCS formation at passage 1. (For interpretation of the references to colour in this figure legend, the reader is referred to the web version of this article.)

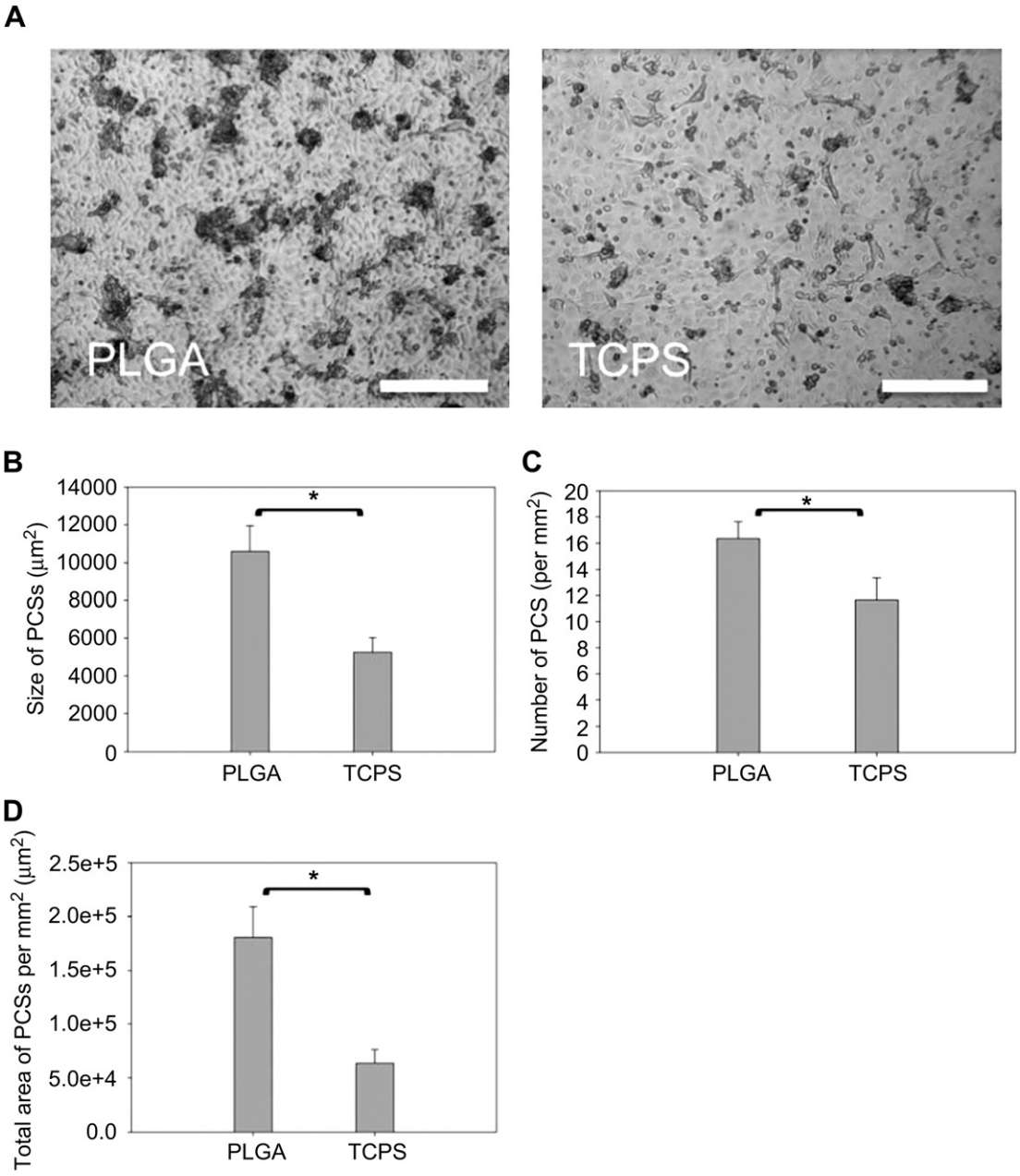

Fig. 3. The different formation tendency on PLGA and TCPS. (A) The light microscopy image of PCSs on PLGA and TCPS after 3 days of high density seeding (1×10^5 cells/cm^2, bar: 200 μm). (B) The comparison of PCS size. (C) The comparison of PCS numbers. (D) The comparison of total area covered by PCSs. Asterisk (*) denotes a significant difference ($p < 0.05$, *t*-test).

number of PCSs on PLGA was about 45% higher than on TCPS (Fig. 3C). The ratio of area covered by PCS on PLGA was about three times larger than on TCPS (Fig. 3D). These results indicate that PLGA possessed higher tendency to facilitate PCS formation than TCPS under the same culture condition.

3.3. Quantification of ECM proteins on PLGA and TCPS

ECM proteins have been extensively studied with respect to substrate adsorption and cellular response [18]. As shown in Fig. 4A, PGAC cells cultured in serum-free medium could secrete fibronectin, which was involved in the ILK pathway and E-cadherin expression regulation [19]. To confirm whether PLGA and TCPS have different ECM protein adsorption ability to influence PCS formation, PLGA and TCPS were incubated with 5 μg/cm^2 fibronectin for 48 h and then the adsorption amount was quantified by Western blot analysis. Fig. 4B shows both PLGA and TCPS have a homogeneous smooth surface without considering surface roughness bias. Fig. 4C shows TCPS exhibited higher adsorption quantity of fibronectin than PLGA. These results indicate that PLGA and TCPS could adsorb different ECM proteins to talk with cultured PGACs.

3.4. Cell migration on PLGA and TCPS

The representative recorded paths traveled by each cell at low density (1×10^4 cells/cm^2) during a 10 h period on PLGA and TCPS were plotted in Fig. 5A. Quantitative comparison showed

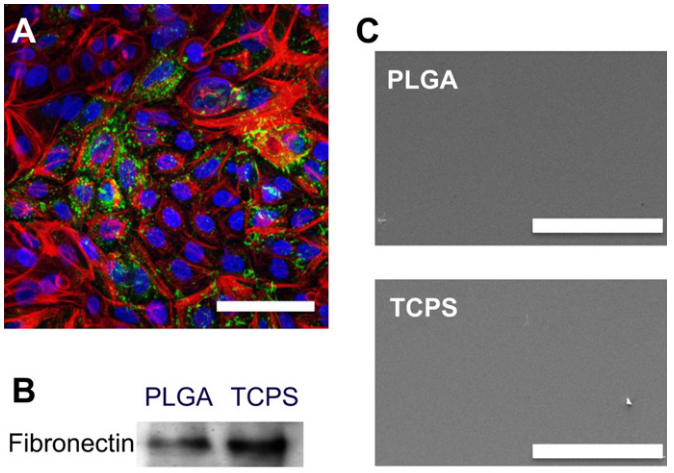

Fig. 4. (A) The immunostaining of fibronectin expression in PGAC cells on TCPS, which showed a random distribution pattern (bar: 25 μm). (B) The Western blot of adsorpted fibronectin on PLGA and TCPS surface. (C) SEM images of PLGA and TCPS surface (bar: 30 μm).

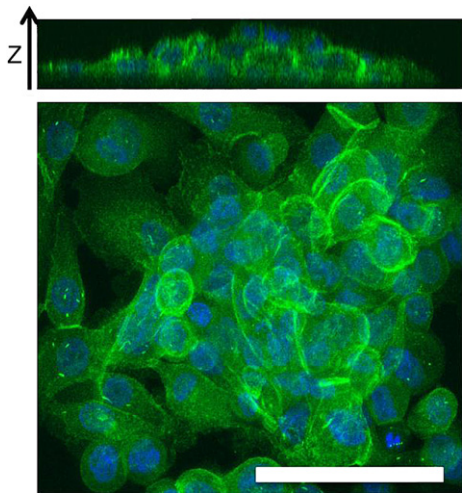

Fig. 6. Distribution E-cadherin molecules in PCS. Compared to the cells at the periphery 2D regions, the E-cadherin expression in PCS cells is slightly stronger (bar: 25 μm).

significant difference in migration velocity of PGAC cells on these two surfaces (Fig. 5B). Averagely, the highest migration velocity of cells on TCPS was about 1.4 times of that on PGLA. Thus, PGAC cells displayed more active random movement on TCPS than on PLGA.

3.5. The role of E-cadherin in PCS formation

The staining for E-cadherin of PGAC cells on TCPS is shown in Fig. 6. PGAC cells showed stronger E-cadherin expression in PCSs, mainly located at the cell borders, than in monolayered cells. The same staining pattern in PCSs was also seen for PGAC cells cultured on PLGA (data not shown). It has been shown that E-cadherin is the major mediator of epithelial cell–cell adhesion [20]. Therefore, it is reasonable to assume that E-cadherin dominated PGAC cell–cell adhesion and further aggregation. To identify this assumption, PGAC cells were seeded on TCPS at low density (1×10^4 cells/cm^2) to prevent the formation of PCS (Fig. 7A). Subsequently, PP1, a specific Src inhibitor, was added to the culture medium to upregulate E-cadherin expression. After 24 h of incubation, consistent with the effect of Src inhibitor, phosphorylated Src levels in PGAC cells were clearly inhibited by PP1 (Fig. 7C). As reported for another cell system [21], when PGAC cells were treated with Src inhibitor, E-cadherin expression was considerably enhanced (Fig. 7C). Interestingly, cell–cell contacts appeared tighter to aggregate (Fig. 7B). Conversely, when PGAC cells were incubated with antibody against E-cadherin, the formation of PCS was disturbed. The area of PCS could be decreased about 33% when 50 μg/ml antibody was added

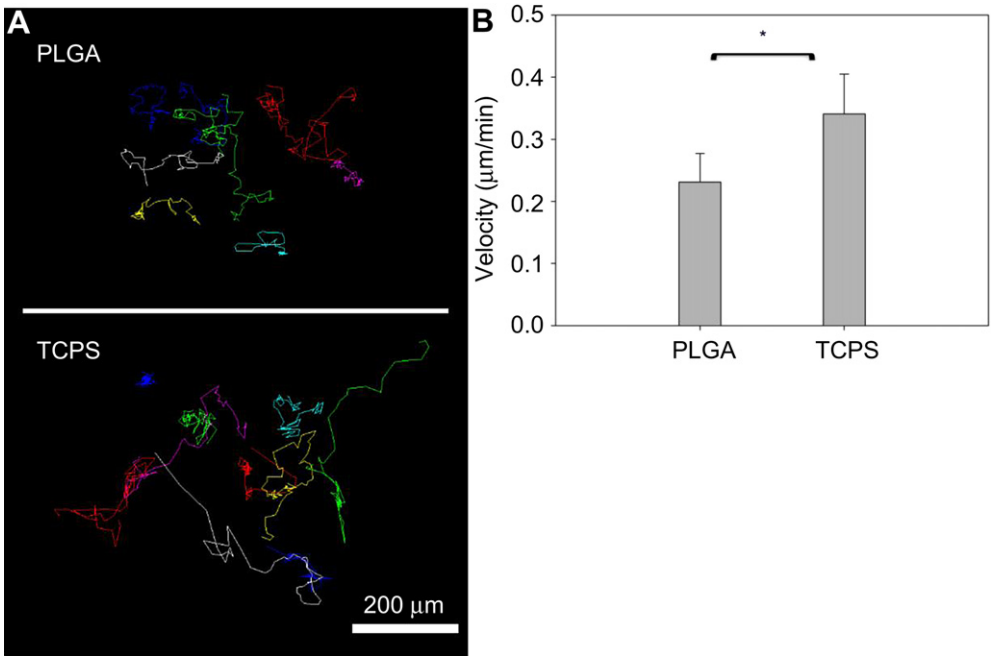

Fig. 5. Cell migration of PGAC cells. (A) Cell migrating trace recorded on PLGA and TCPS (bar: 200 μm) of 10 individual PGAC cells. (B) The comparison of highest 10% velocity records on PLGA and TCPS. * denotes a significant difference ($p < 0.01$, t-test).

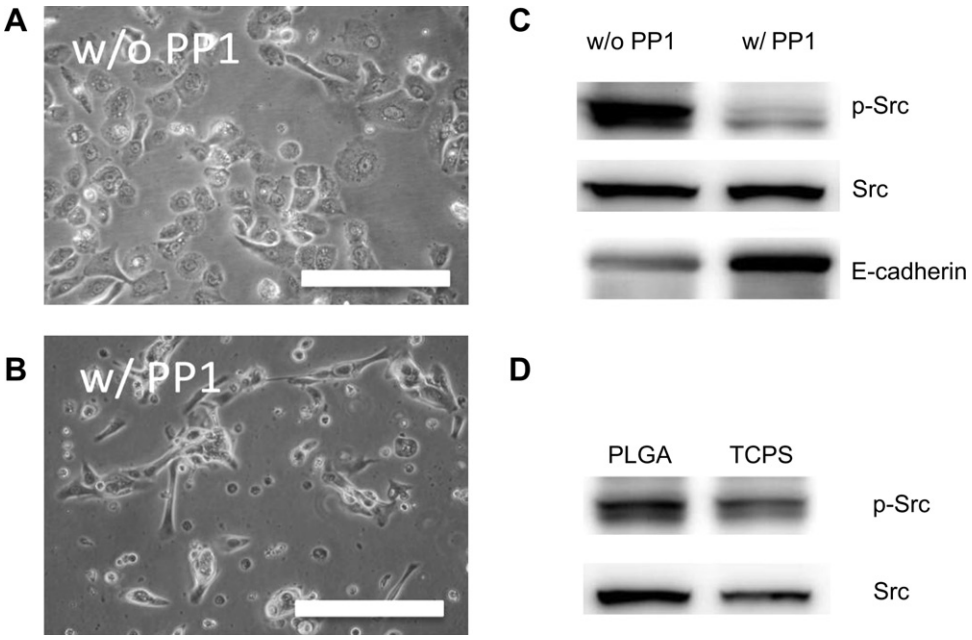

Fig. 7. The effect of addition Src inhibitor PP1 on cell aggregation. (A) The cells seeded at 1×10^4 cells/cm^2 did not form PCS. (B) At the same time, those cells that were treated with PP1 were found to form aggregation on TCPS (bar: 100 μm). (C) Western blot analysis of p-Src, Src, and E-cadherin. The p-Src was successfully inhibited by PP1, and E-cadherin was up-regulated. (D) Western blot of PGAC cells on PLGA and TCPS. The band of p-Src on TCPS showed a slightly decrease compared to that of PLGA.

into the culture medium. These results suggest that E-cadherin may be involved in the process of PGAC cell aggregation and the PCS formation.

3.6. *The role of PLGA on activating E-cadherin signaling pathway to mediate PCS formation*

To investigate the effect of substrates on the cytoskeleton and focal contacts, PGACs were cultured on PLGA and TCPS for 3 days and then subjected to actin and vinculin staining. As shown in Fig. 8A, cells grown on TCPS contained obvious focal contact structures at the cell periphery and longitudinal actin stress fibers. In contrast, actin stress fibers were less organized and the focal contacts were seldom found in cells cultured on PLGA. In addition, cytosolic staining of vinculin was observed on PLGA. These findings suggest that the formation of PCS in PGAC cells might be closely related to actin cytoskeleton organization, focal adhesions between the cell and the extracellular matrix (ECM), and the related downstream signal transductions. Those factors were also related to the cell-substrate adhesion strength. Subsequently, we examined whether TCPS had the tendency to promote cell-substrate adhesion. In cell attachment assay, the levels that $66 \pm 9\%$ and $87 \pm 3\%$ of total seeded cells attached to PLGA and TCPS were achieved after 4 h, respectively (Fig. 8B). Thus, PLGA was less effective in PGAC cell attachment than TCPS. Similarly, cells were removed easier on PLGA by trypsin treatment for 60 s, a common method for recovering cells from substrates. Approximately $17 \pm 4\%$ and $56 \pm 5\%$ of total initial seeded cells were still could be counted on the substrate surface, respectively (Fig. 8C). These results revealed TCPS led to a significant enhancement of PGAC cell adhesion to the substrate. In other words, TCPS had stronger adhesion force than PLGA.

Previous study has demonstrated that the exogenous expression of ILK and Snail in epithelial cells results in the dramatic down-regulation of E-cadherin [22]. Consistent with previous works, Fig. 9 shows E-cadherin expression of PGAC cells on PLGA was up-regulated in protein and genetic analysis by the decreased expression of ILK and Snail. However, the extent of Src phosphorylation was higher on PLGA than on TCPS (Fig. 7D). It was contrary to the PP1 effect shown in Fig. 7C, in which the higher phosphorylation of Src led in the lower E-cadherin expression. Therefore in this case, the Src pathway did not regulate the difference of E-cadherin expression on PLGA and TCPS.

4. Discussion

Human salivary gland epithelial cells are at a highly differentiated status so it is important to require a significant amount of primary salivary gland cells and to characterize the physiological property of cultured cells. In our previous study [5], human PGAC cells have been successfully isolated and expanded by using K-SFM-based medium (Fig. 1) and cells in over-crowded regions could form three-dimensional PCSs to exhibit higher expression levels and different location patterns of function-related proteins compared to the 2D cells (Fig. 2). This is consistent with previous studies that 3D culture systems can mimic the in vivo environment for acinar cells to recover their function. For example, it has also been shown that the ability of hair follicle induction of dermal papilla cells [17], albumin production of hepatocytes [23], dopamine secretion of PC12 cells [24] are enhanced when they are cultured into 3D aggregates.

A number of methods can be employed to culture cells into 3D aggregates. The simplest way is to maintain cells in spinner flasks where the culture system is continuously rotated, thereby preventing cells from adhering to the culture vessel. Another in vitro method of inducing 3D structures involves culturing cells within a gel system. When cells are seeded in gels, their movement may be confined and grow into dense aggregates. Third, cell aggregates can also be obtained by direct scraping under high cell densities. However, these methods do not allow investigation of the cell self-assembly process. Therefore, in the present study, we disclose the feasibility of using the FDA-approved biomaterial PLGA to culture PGAC cells for promoting the formation of three-dimensional PCS. Compared to TCPS, PLGA can facilitate PCS formation, both in the sizes and the numbers (Fig. 3).

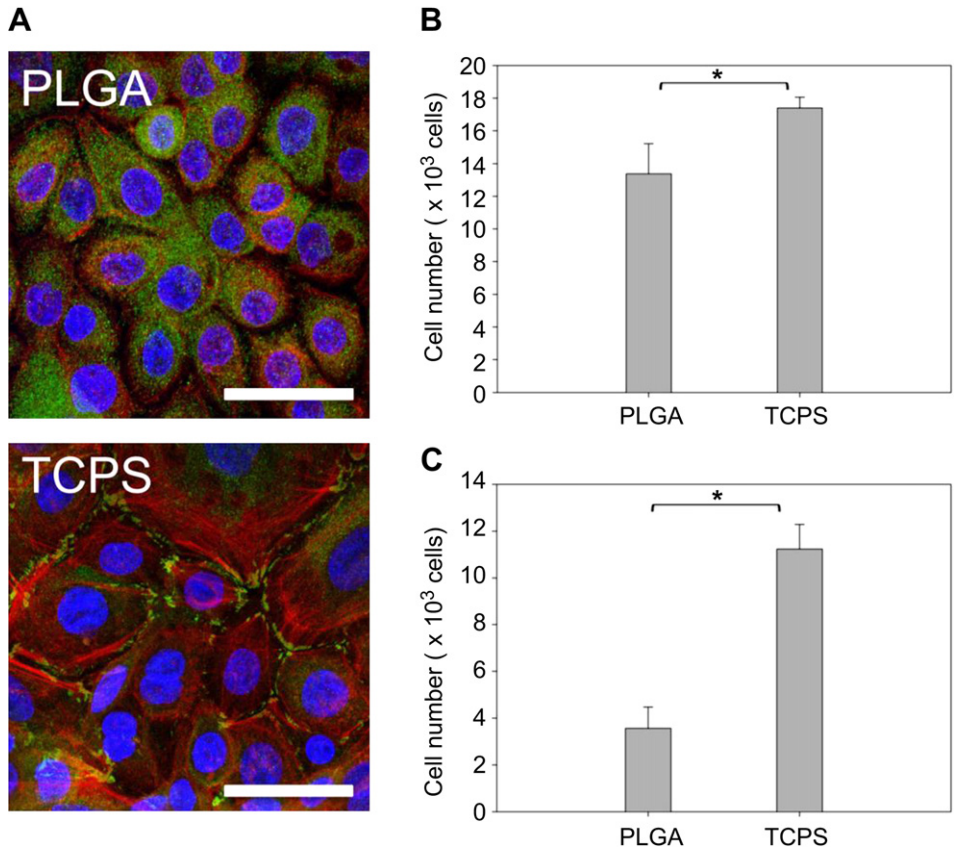

Fig. 8. The cell-substrate adhesion. (A) Confocal imaging of staining focal contact structures on PLGA and TCPS. (Bar, 15 μm. Red: F-actin. Green: Vinculin. Blue: Nuclei.). (B) The Initial cell attaching rate on PLGA and TCPS. The initial cell seeding density was 2×10^4 cells. (C) The remaining cell numbers on substrate after 1 min of trypsinization. (For interpretation of the references to colour in this figure legend, the reader is referred to the web version of this article.)

It is reasonable to assume that cells form 3D structure on a 2D surface via migration after close intercellular contact can be reached. We may envision the rate-determining steps of PCS formation to be either the rate of cell migration to the PCS surface (migration control by cell-substrate interaction) or the rate of adhesion of cell to the PCS surface (adhesion control by cell–cell interaction). Straightforwardly, the higher cell migration rate the more possibility for cell–cell contact, so the formation of more PCSs can be expected. Based on this assumption, PLGA should be able to promote PGAC cell migration to form more and lager PCSs than TCPS. However, Fig. 5 shows PGAC cells displayed more active random movement on TCPS than on PLGA. Therefore, cell migration may not be essential for the formation of PCS on PLGA. This is consistent with the fact that PCS was observed after PGAC cells reached confluence.

In addition to the dynamics of cell migration, another possibility accounting for the formation of PCS is that the static force of cell–cell interaction is able to provide strong intercellular adhesion. The factors affecting cell–cell interaction includes the trophic factors, serum factors, integrins, and adhesions molecules. It has been shown that E-cadherin is the major mediator for cell cohesion [25]. As shown in Fig. 6, obvious E-cadherin pattern alongside the cell boundary within 3D PCS was observed. Thus, we proposed that surface adhesion molecules, especially E-cadherin, may play an important role in mediating homophilic intercellular binding during the process of PCS formation. If this is the case, the enhancement of E-cadherin expression may be beneficial for the formation of PCS and the inhibition of E-cadherin expression is able to retard the formation of PCS.

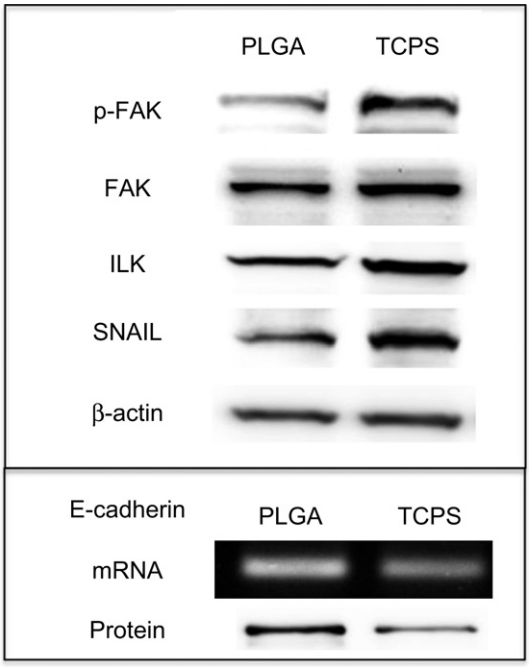

Fig. 9. The Western bolt analysis of Integrin β1, p-FAK, FAK, ILK, Snail, E-cadherin, and mRNA expression of E-cadherin.

The observation that Src signaling induces a switch in adhesion type predominance from cadherin- to integrin-based adhesions [26] leads us to hypothesize that Src activity could have an opposite role in E-cadherin-mediated PCS formation. Certainly, we demonstrated that the Src inhibitor PP1 exactly caused up-regulation of E-cadherin protein in PGAC cells and enhanced cell–cell adhesiveness in a low-seeding-density cell aggregation assay (Fig. 7). Furthermore, PGAC treated with antibody against E-cadherin abolished the formation of PCS. These results suggest that the decision of PGAC cells to initiate PCS formation requires the formation of E-cadherin cell–cell junctions. Hence, the static force of homophilic interaction on surfaces of individual cells, but not the dynamics of cell migration, may play a more important role in PCS formation.

We next asked whether biomaterial could play a role in the E-cadherin-dependent cell adhesion to mediate PCS formation. It is known the cell–biomaterial interaction is of extreme importance in regulating the numerous functions necessary for cell adhesion, growth and differentiation. The direct contact between cell and substrate is the first step for cell adhesion onto the substrate, but it is generally considered to be a multistep process involving adsorption of ECM proteins onto the substrate surface and recognition of ECM components by cell surface receptors, followed by cytoskeletal rearrangements that lead to cell spreading [27,28]. Indeed, the fibronectin adsorption test in Fig. 4 reveals that PLGA and TCPS had different ECM adsorption ability in this study.

Among cell surface receptors, integrin receptor is mainly responsible for cell-ECM interactions to induce the formation of focal adhesions and to generate a cascade of phosphorylation of signal transduction molecules to modulate signaling pathways. Focal adhesion kinase (FAK) is located at focal contact and plays a key role in regulating cell spreading and migration. On the other hand, the role of integrin-linked kinase (ILK) has been found to interact with β1 and β3 integrins and to transduce signals from ECM components to downstream signaling components [19]. The activation of ILK in epithelial cells has been shown to result in loss of cell–cell adhesion, due to the down-regulation of E-cadherin expression [19]. The down-regulation of E-cadherin expression also involves ILK-mediated activation of the E-cadherin suppressor, snail [29]. Thus, interaction between integrin and ECM proteins also modulates snail phosphorylation [30]. Based on these previous studies, we hypothesize that biomaterials can modulate the PCS formation in PGAC cells via the ligand-binding of integrins, ILK signaling pathway, and regulation of the E-cadherin expression [22].

In this study, PGAC cells on TCPS showed more developed focal adhesion contacts and more effective cell attachment than those on PLGA (Fig. 8). By Western blot analysis, PLGA mediated lower p-FAK and ILK expression of PGAC cells, which in turn regulates the expression of snail and E-cadherin with a reciprocal relationship (Fig. 9). Since PGAC cells were found to have a greater tendency to form PCS on PLGA than on TCPS (Fig. 3), our data demonstrate that biomaterial can support PGAC cells to form more PCS through the effects on enhancing E-cadherin expression, which is associated with the suppression of FAK/ILK/snail in PGAC cells. Thus, selective appropriate biomaterials may be potentially useful in generating PCS and recover epithelial characteristics.

On the other hand, since inhibition of Src also resulted in stimulating E-cadherin expression, we examined whether the expression of E-cadherin could be regulated by Src, on different biomaterials. However, as shown in Fig. 7D, this does not seem to be the case, since phosphorylation of P38 (data not shown) and Src had no significant difference for PGAC cells cultured on PLGA or TCPS. Thus, Src signaling pathway is likely not involved in the biomaterial-stimulated E-cadherin expression.

By the way, it is known that the conversion of an epithelial cell to a mesenchymal cell is a crucial step of tumorigeneses. The hallmarks for the epithelial to mesenchymal transformation (EMT) have been associated with the loss of epithelial phenotype, increased fibronectin matrix deposition, production of transcription factor snail able to inhibit E-cadherin expression, and activation signaling molecules such as FAK and ILK [30–32]. Interestingly, this study suggests that E-cadherin can be considered to have an opposite role in PCS formation and EMT. Thus, application of biomaterial may also lead to another way of restoring the frequently observed down-regulation of E-cadherin expression in many types of carcinomas.

5. Conclusion

When PGAC cells were cultured on PLGA, higher level of PCS formation was observed than on TCPS. This different formation tendency was regulated by the differential expression of E-cadherin molecules on both substrates. PLGA provided a more weaker cell-substrate adhesion for PGAC cells and serially down-regulated the downstream FAK, ILK, and Snail expression; however, the descending of Snail reversibly enhanced the endogenous E-cadherin expression, finally lead into a stronger cell–cell adhesion and the higher level of PCS formation. This study revealed the possibility of controlling cell aggregation behaviors by choosing different biomaterials.

Acknowledgement

The authors thank National Science Council of the Republic of China for their financial support of this research. This work is supported in part by the National Science Council of the Republic of China (NSC99-2628-B-002-050 MY3) to P-J Lou.

References

[1] Aframian DJ, Palmon A. Current status of the development of an artificial salivary gland. Tissue Eng Part B Rev 2008;14:187–98.
[2] Okura M, Shirasuna K, Hiranuma T, Yoshioka H, Nakahara H, Aikawa T, et al. Characterization of growth and differentiation of normal human submandibular gland epithelial cells in a serum-free medium. Differentiation 1993; 54:143–53.
[3] Sabatini LM, Allen-Hoffmann BL, Warner TF, Azen EA. Serial cultivation of epithelial cells from human and macaque salivary glands. In Vitro Cell Dev Biol 1991;27A:939–48.
[4] Kurth BE, Hazen-Martin DJ, Sens MA, DeChamplain RW, Sens DA. Cell culture and characterization of human minor salivary gland duct cells. J Oral Pathol Med 1989;18:214–9.
[5] Chan YH, Huang TW, Young TH, Lou PJ. Selective culture of different types of human parotid gland cells. Head Neck 2011;33(3):407–14.
[6] Zhu Y, Aletta JM, Wen J, Zhang X, Higgins D, Rubin RP. Rat serum induces a differentiated phenotype in a rat parotid acinar cell line. Am J Physiol 1998; 275:G259–68.
[7] Aframian DJ, Tran SD, Cukierman E, Yamada KM, Baum BJ. Absence of tight junction formation in an allogeneic graft cell line used for developing an engineered artificial salivary gland. Tissue Eng 2002;8:871–8.
[8] Bucheler M, Wirz C, Schutz A, Bootz F. Tissue engineering of human salivary gland organoids. Acta Otolaryngol 2002;122:541–5.
[9] Hiraki A, Shirasuna K, Ikari T, Shinohara M, Garrod DR. Calcium induces differentiation of primary human salivary acinar cells. J Cell Physiol 2002;193: 55–63.
[10] Okumura K, Nakamura K, Hisatomi Y, Nagano K, Tanaka Y, Terada K, et al. Salivary gland progenitor cells induced by duct ligation differentiate into hepatic and pancreatic lineages. Hepatology 2003;38:104–13.
[11] Joraku A, Sullivan CA, Yoo JJ, Atala A. Tissue engineering of functional salivary gland tissue. Laryngoscope 2005;115:244–8.
[12] Tran SD, Sugito T, Dipasquale G, Cotrim AP, Bandyopadhyay BC, Riddle K, et al. Re-engineering primary epithelial cells from rhesus monkey parotid glands for use in developing an artificial salivary gland. Tissue Eng 2006;12:2939–48.
[13] Qi B, Fujita-Yoshigaki J, Michikawa H, Satoh K, Katsumata O, Sugiya H. Differences in claudin synthesis in primary cultures of acinar cells from rat salivary gland are correlated with the specific three-dimensional organization of the cells. Cell Tissue Res 2007;329:59–70.
[14] Chan YH, Huang TW, Young TH, Lou PJ. Human salivary gland acinar cells spontaneously form three-dimensional structures and change the protein expression patterns. J Cell Physiol 2011;226:3076–85.

[15] Chen RS, Chen YJ, Chen MH, Young TH. The behavior of rat tooth germ cells on poly(vinyl alcohol). Acta Biomater 2009;5:1064–74.
[16] Lin S, Jee S, Hsaio W, Lee S, Young T. Formation of melanocyte spheroids on the chitosan-coated surface. Biomaterials 2005;26:1413–22.
[17] Young TH, Lee CY, Chiu HC, Hsu CJ, Lin SJ. Self-assembly of dermal papilla cells into inductive spheroidal microtissues on poly(ethylene-co-vinyl alcohol) membranes for hair follicle regeneration. Biomaterials 2008;29: 3521–30.
[18] Whitelock JM. Adhesion of cells to biomaterials. Encyclopedia of biomedical engineering. New Jersey: Wiley Publishing Inc; 2006. pp. 1–8.
[19] Wu C, Keightley SY, Leung-Hagesteijn C, Radeva G, Coppolino M, Goicoechea S, et al. Integrin-linked protein kinase regulates fibronectin matrix assembly, E-cadherin expression, and tumorigenicity. J Biol Chem 1998;273: 528–36.
[20] Tsuchiya B, Sato Y, Kameya T, Okayasu I, Mukai K. Differential expression of N-cadherin and E-cadherin in normal human tissues. Arch Histol Cytol 2006;69: 135–45.
[21] Nam J, Ino Y, Sakamoto M, Hirohashi S. Src family kinase inhibitor PP2 restores the E-cadherin/catenin cell adhesion system in human cancer cells and reduces cancer metastasis. Clin Cancer Res 2002;8:2430–6.
[22] Oloumi A, McPhee T, Dedhar S. Regulation of E-cadherin expression and beta-catenin/Tcf transcriptional activity by the integrin-linked kinase. Biochim Biophys Acta 2004;1691:1–15.
[23] Lu JN, Wang CC, Young TH. The behaviors of long-term cryopreserved human hepatocytes on different biomaterials. Artif Organs 2011;35:E65–72.
[24] Young TH, Hung CH. Change in electrophoretic mobility of PC12 cells after culturing on PVA membranes modified with different diamines. J Biomed Mater Res 2003;67A:1238–44.
[25] van Roy F, Berx G. The cell-cell adhesion molecule E-cadherin. Cell Mol Life Sci 2008;65(23):3756–88.
[26] Palacios F, Tushir J, Fujita Y, D'Souza-Schorey C. Lysosomal targeting of E-cadherin: a unique mechanism for the down-regulation of cell-cell adhesion during epithelial to mesenchymal transitions. Mol Cell Biol 2005;25:389–402.
[27] Clark E, Brugge J. Integrins and signal transduction pathways: the road taken. Science 1995;268:233–9.
[28] Miyamoto S, Teramoto H, Coso O, Gutkind J, Burbelo P, Akiyama S, et al. Integrin function - molecular hierarchies of cytoskeletal and signaling molecules. J Cell Biol 1995;131:791–805.
[29] Tan C, Costello P, Sanghera J, Dominguez D, Baulida J, de Herreros AG, et al. Inhibition of integrin linked kinase (ILK) suppresses beta-catenin-Lef/Tcf-dependent transcription and expression of the E-cadherin repressor, snail, in APC-/- human colon carcinoma cells. Oncogene 2001;20:133–40.
[30] Nieto M. The snail superfamily of zinc-finger transcription factors. Nat Rev Mol Cell Bio 2002;3:155–66.
[31] Radeva G, Petrocelli T, Behrend E, LeungHagesteijn C, Filmus J, Slingerland J, et al. Overexpression of the integrin-linked kinase promotes anchorage-independent cell cycle progression. J Biol Chem 1997;272:13937–44.
[32] Somasiri A, Howarth A, Goswami D, Dedhar S, Roskelley C. Overexpression of the integrin-linked kinase mesenchymally transforms mammary epithelial cells. J Cell Sci 2001;114:1125–36.